INIS

Theoretical and Experimental Study of the crash of a model of an irradiated fuel container

J 6/8

S. GOLDSTEIN

C.E.A. - Département des Etudes Mécaniques et Thermiques

CEN - SACLAY B.P. n°2 - 91190 GIF-SUR-YVETTE

J. FRADIN

C.O.G.E.M.A. - CEN - FONTENAY-AUX-ROSES

B.P. n°6 - 92260 FONTENAY-AUX-ROSES

R. LABROT

C.E.A. - C.E.S.T.A.

B.P. n°2 - 33114 LE BARP

4. International conference on structural mechanics in reactor engineering. San Francisco, Calif., USA 15-19 August 1977

CEA-CONF--4061

FR7800318

1. Introduction

This study concerns the safety of the transport of irradiated fuel containers - To be approved a container must satisfy severe conditions such as resistance to fire and shock tests. During transportation, it is covered by a shock absorber casing, to be protected against accidental shocks. During handling within the reactor containements, this casing is removed and it is then feared that after an accidental crash a loss of protection or tightness may occur. Crash tests with 1/5 scale models without casing have been performed at the Centre d'Etudes Scientifiques et Techniques d'Aquitaine (C.E.S.T.A. - C.E.A. BORDEAUX).

The salient features of these tests are described in § 2, i e : description of the models, instrumentation and results. The numerical interpretation is discussed in § 3; it arises difficulties coming from internal contact non linearities, constitutive laws of the materials and modelisation.

2. Description of the experiments

2.1 Description of the models

The 1/1 scale container is designed in order to contain 12 PWR fuel element clusters; its weight is 100 tons. The tested 1/5 scale model weights 800 kgs; its internal structure can be seen on the meridian cross section represented on fig. 1. It is made of :

- An external stainless steel vessel 6 mm thick
- A thermal protection of plaster compound 165 mm thick
- A lead protection of 200 mm thick
- An internal stainless steel vessel 5 mm thick
- An upper and a lower circular flange for mechanical protection during handling.

The plug which is made of the same materials is fixed on the top with 24 screws. The fuel element clusters were simulated by an internal rigid load of 80 kgs.

2.2 Instrumentation

2.2.1. Metrology

Overall dimensions of the models have been measured before and after the crashes. Regularly spaced lines have been drawn on the lead and the vessels to give an estimation of the local plastic deformations. Absolute accuracy on ± 1% can be reached by this metho

2.2.2. Accelerometers

Twelve accelerometers have been implemented on the models as shown on fig.1. : A1 to A4 on the external vessel, A5 on the plug, A7 to A10 on the internal vessel and A11 and A12 on the lead. Except A5 and A6, they weve arranged symetrically by pairs in order to collec mean values of the the axial deformations.

2.2.3. Films

Films at five thousands frames per second have been taken during each test. From these films, displacement versus time curves could be drawn which corroborated the responses of accelerometers A2 and A3.

.../...

2.3 Description of the experiments

2.3.1. 10 m high flat drop

The aim of this first prudent drop was to test the experimental apparatus and to be able to make preliminary numerical comparisons for a not much deformed model. The following observations could be made after this first test :

A slight fissure appeared at the welding of the bottom (Cf. fig.1)

- The lead protection slipped on the internal vessel allowing a gap at its upper part.
- The lower part of the external vessel exhibited two swellings a major one under the flange and a much less important one above the flange.
- The lead remained cylindrical and its axial deformation was almost homogeneously spead.

These typical deformations are shown on fig. 2, 3 and 4 and numerical values of some selected deformations are reported in table 1. Peak values of the recorded accelerations reached about 3000 g for the accelerometers fixed on the steel structures (A1 to A10), and about 500 g for A11 and A12 fixed on the lead. Velocity and displacements as functions of time could be obtained by successive integrations of these signals. The relative permanent displacements between the accelerometers thus obtained were in good agreement with those measured with the help of the films and those measured on the model after the crashes. The strain gauges revealed very slight elastic deformations (extensions) on the internal vessel (400 to 800 10^{-6}). Those stuck on the lower part of the external vessel indicated deformations which where inconsistent with those resulting from the metrology, and probably came unstuck.

For this test, the target on which this first model fell was not perfectly rigid. It was made of a very thick slab supported on its edges and which could bend up to 1 cm. As a consequence a discrepancy concerning the duration of the impact appeared between calculation and experiment. Concrete has been poured in the gap under the slap for the next crashes and a better fitting could be reached.

2.3.2. 27 m high flat drop

On the whole the same observations as for the first test could be made, with increasing values of deformations and accelerations (peak values of 8000 g). However accelerometer A5 (Fig. 5) indicated two sharp negative peaks. The second one at 2,2 ms is probably due to the striking of the plug by the internal load; as a matter of fact the plug remained curved outwards.

2.3.3. 27 m high tilt drop

No measurements were made during this experiment which was intended to test the crushing-strength of the model to more severe conditions. As it will be seen on the film, the model rebounded and turned over in the air. A large opening located at the welding lines appeared in the external vessel.

3. Numerical interpretation

3.1. Description of the PASTEL code

The small deformation plastic-dynamic option of the code solves the following basic equation :

$$M\ddot{X} + KX = F(t) + F^{p}(t) \qquad (1)$$

.../...

where M is the mass-matrix, K the stiffness matrix F (t) the external load and $F^P(t)$ the plastic nodal forces.

h being the time step, (1) is discretised according to the central difference scheme :

$$(2)\quad \left(M + \frac{h^2}{4}K\right)\begin{pmatrix} I & 0 \\ 0 & I \end{pmatrix}\begin{pmatrix} \dot{X}_{n+1} \\ X_{n+1} \end{pmatrix} = \begin{pmatrix} M - \frac{h^2}{4}K & -hK \\ \frac{h}{4}M & M - \frac{h^2}{4}K \end{pmatrix}\begin{pmatrix} \dot{X}_n \\ X_n \end{pmatrix} + h\begin{pmatrix} \frac{F_n + F_{n+1}}{2} \\ \frac{h}{4}\frac{F_n + F_{n+1}}{2} \end{pmatrix}$$

where I and 0 are identity and null matrices $\dot{X}$ and X the nodal velocities and displacements, subscripts n and n+1 correspond to time t and t+h, $F_n = F(t) + F^P(t)$, and $F_{n+1} = F(t+h) + F^P(t+h)$. Constant stiffness plastic iterations are performed to calculate $F^P(t+h)$. These nodal forces are calculated with the increment $\Delta\underset{\sim}{\varepsilon}^P$ of the plastic flow tensor $\underset{\sim}{\varepsilon}^P$. $\Delta\underset{\sim}{\varepsilon}^P$ is calculated implicitly by solving the following equations

$$(3)\quad \underset{\sim}{\sigma}^i = D\left(\underset{\sim}{\varepsilon}^i - \underset{\sim}{\varepsilon}^P_n - \Delta\underset{\sim}{\varepsilon}^P\right) \qquad \text{stress-strain relation}$$

$$(4)\quad \Delta\underset{\sim}{\varepsilon}^P = \delta\lambda \frac{\partial f}{\partial \underset{\sim}{\sigma}^i} \qquad \text{if load}$$

$$\Delta\underset{\sim}{\varepsilon}^P = 0 \qquad \text{if unload}$$

$$(5)\quad f(\sigma^i) = g(\lambda + \delta\lambda) \qquad \text{hardening rule}$$

where $\underset{\sim}{\varepsilon}^i, \underset{\sim}{\sigma}^i$ are the total deformation and stress tensors at iteration i, and $f(\underset{\sim}{\sigma})$ the yield criterium. $\underset{\sim}{\sigma}^i$ is calculated from (3), (4) and (5) with given $\underset{\sim}{\varepsilon}^i$ and $\underset{\sim}{\varepsilon}^P_n$ with the help of internal iterations.

Von Mises yield criterium have been used for lead and steel and Drücker-Prager [1] for the plaster compound i-e :

$$(6)\quad f(\sigma) = \alpha I_1 + \beta\sqrt{I_2} - 1 \qquad \text{if} \qquad I_1 \geq -\sqrt{I_2}$$

$$(7)\quad f(\sigma) = \beta\sqrt{I_2} - 1 \qquad \text{if} \qquad I_1 \leq -\sqrt{I_2}$$

where I_1 and I_2 are the two invariants of the deviatoric stress tensor and α and β numerical coefficients fitted on the ultimate stregths in tension and compression. As a matter of fact the plaster compound was almost everywhere in compression during the transient and (7) was most commonly applied. The yield stress beeing very low and the material perfectly plastic, the plaster compound acted as a liquid incompressible material.

3.2. Modelisation of the structure

The modelisation is showed on fig.6 where some particular node numbers used in table 1 are reported. Due to several unilateral contact non linearities three modelisations have been tested.

Modelisation 1

The vessels have been meshed with membrane elements (acting only in traction and compression, without bending) and the weight of the internal load was numerically spread on the bottom of the container.

Modelisation 2

Same as mod.1 except the fact that nodes 5-10-15-20 and 25 (fig.6) have the same vertical displacements i-e the bottom of the internal vessel is rigid.

Modelisation 3

[illegible] except the cylindrical part of the internal vessel has only a

circumferential stiffness and no vertical stiffness i-e the membrane elements are replaced by nodal ring elements. Moreover very soft elements have been introduced at the upper part of the lead. This modelisation allows the lead to slip downwards without friction and is best suited to calculate the breadth of the gap mentioned in § 2.3.1.

3.3. Numerical results

Overall permanent deformation are reported in table 1. The results obtained with the preceding models are compared to the experience for the 10 m drop while only computations with mod.2 have been run for the 27 m flat drop.

$\delta y_{41} - \delta y_{230}$ is the overall shortening of the model. With regard to mod.3 the lead is disconnected from the external vessel and the figure is lower than that of mod.1. The experimental value i-e 16 mm is obtained by double integration of A5 accelerometer signal. The value measured directly on the deformed model is comprised between 15 mm and 20 mm. For the 27 m high drop the predicted value is larger than the experimental one, because of the striking of the plug by the internal load (Cf. fig. 13). Next figures in table 1 show that the agreement is not so good for what concerns the lower part of the external vessel (buckling on both sides of the flange). The calculated deformations are less concentrated than the experimental ones. In particular δ x 44 = 11 to 13,2 VS 18 mm and 22 mm VS 30 mm and $\delta y_{41} - \delta y_{60}$ = 9,5 to 11,6 VS 16,7 mm and 18,4 VS 44 mm. With regard to the lead deformation mod.3 should be best suited. $\delta y_{221} - \delta y_{218}$ is the breadth of the gap shown on Fig.2 : 10,7 VS 12 mm.

$\delta y_{30} - \delta y_{218}$ is the overall shortening of the load : 22,3 mm VS 15 mm. In return the elephant paw shape of the lead seems to be better calculated for the 27 m high drop. Displacement versus time curves are shown together on fig.7, 8 and 9 for the 10 m drop and accelerometers A3, A5 and A11.

It can be noticed a discrepancy concerning the duration of the impact probably due to the fact that the target was not perfectly rigid. Fig.10 shows typical deformations obtained with the calculation. Fig.11 to 14 show similar curves for the 27 m plat drop. In this case the slope of the curves are in very good agreement. The striking of the plug by the internal load can be seen on fig.13.

4. Conclusion

The three drop tests mentioned above have shown that in all cases the tightness of the models was preserved and no loss of protection occured for this design of container. The calculations are in relatively good agreement for what concerns overall deformations and deformation rates except for the buckling of the external vessel. This point will be resumed by using shell elements and large displacement theory.

References

1 D. DRUCKER, W. PRAGER - Q. Appl. Math 10, 157-165 (1952)

- TABLE 1 -

DEFORMATIONS	10 METERS DROP				27 METERS DROP	
	Mod. 1	Mod.2	Mod.3	Experience	Modele 2	Experience
External vessel :						
$(\delta y_{41} - \delta y_{230})$	23,2	21,4	18,6	16 *	53,8	41,8 *
$(\delta y_{41} - \delta y_{60})$	11.6	10,5	9,5	16,7 *	18,4	44 *
$(\delta y_{41} - \delta y_{120})$	20,4	19,4	18	16,5 *	45,5	46 *
δx_{44}	13,2	13	11	18	22	30
δx_{105}	1	0,93	1,4	0,6	4,5	1
lead :						
$(\delta y_{41} - \delta y_{193})$	22	20,9	35,2	25,3 *	54	73 *
$(\delta y_{221} - \delta y_{218})$	1,05	0,64	10,7	12	0,68	30
$(\delta y_{30} - \delta y_{218})$	12,7	14,1	22,3	16	43	44
δx_{34}	10,8	10	7,49	1	16,8	10
$(\delta y_{3} - \delta y_{5})$	1,2	1	1	0	6,1	4
δx_{103}	0,5	0,5	0,7	0,5	1,9	1,9

* Double integration of the accelerometer signals.

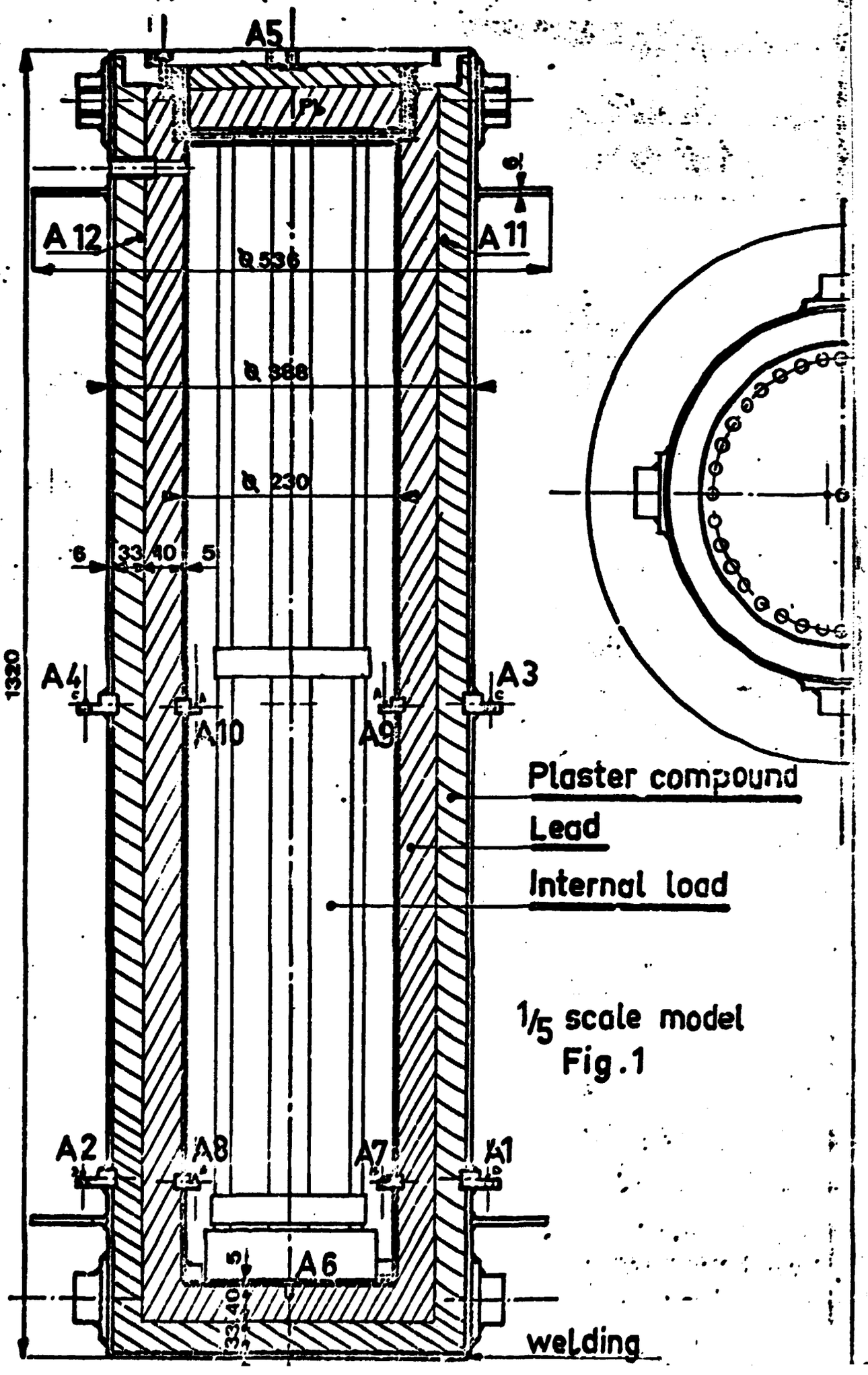

1/5 scale model
Fig. 1

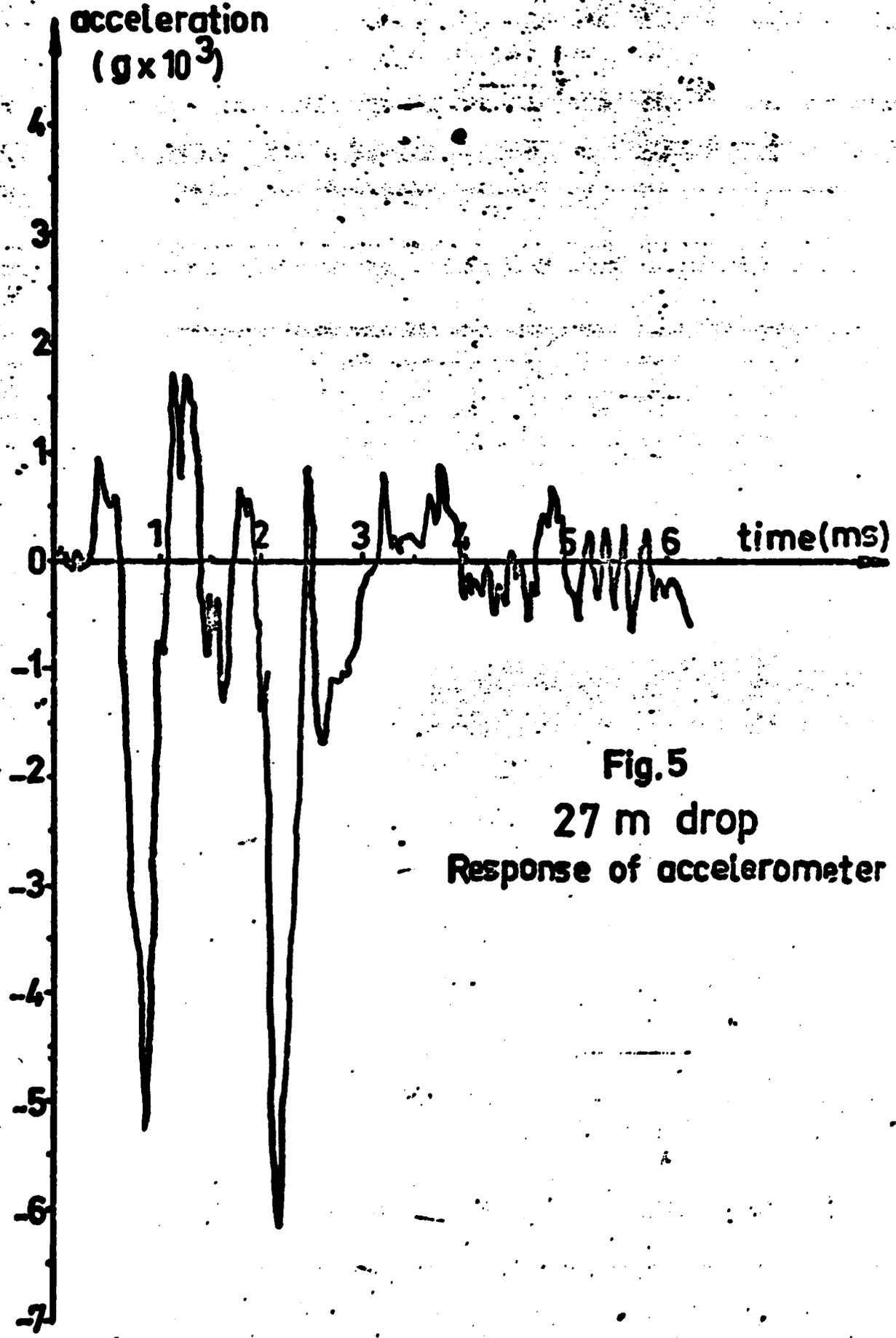

Fig.5

27 m drop

Response of accelerometer A5

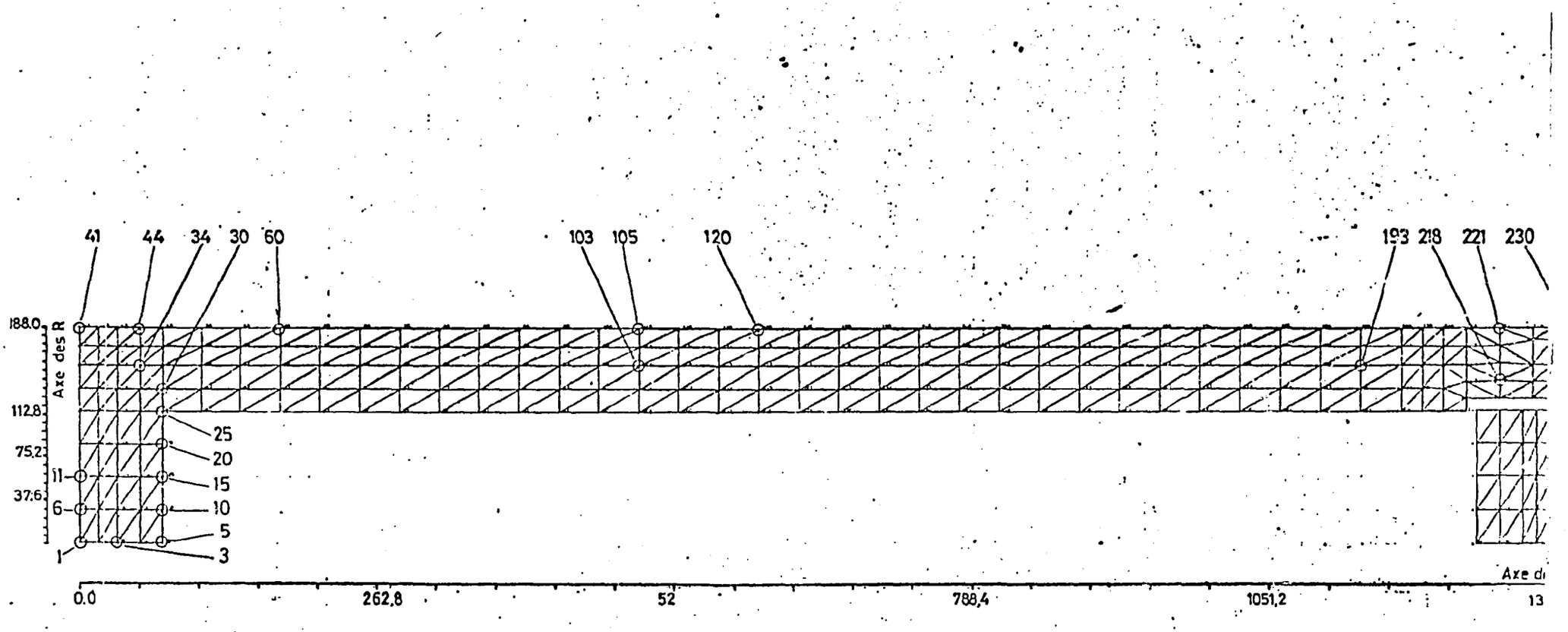

Nodes numbers

Fig.6

Fig. 7

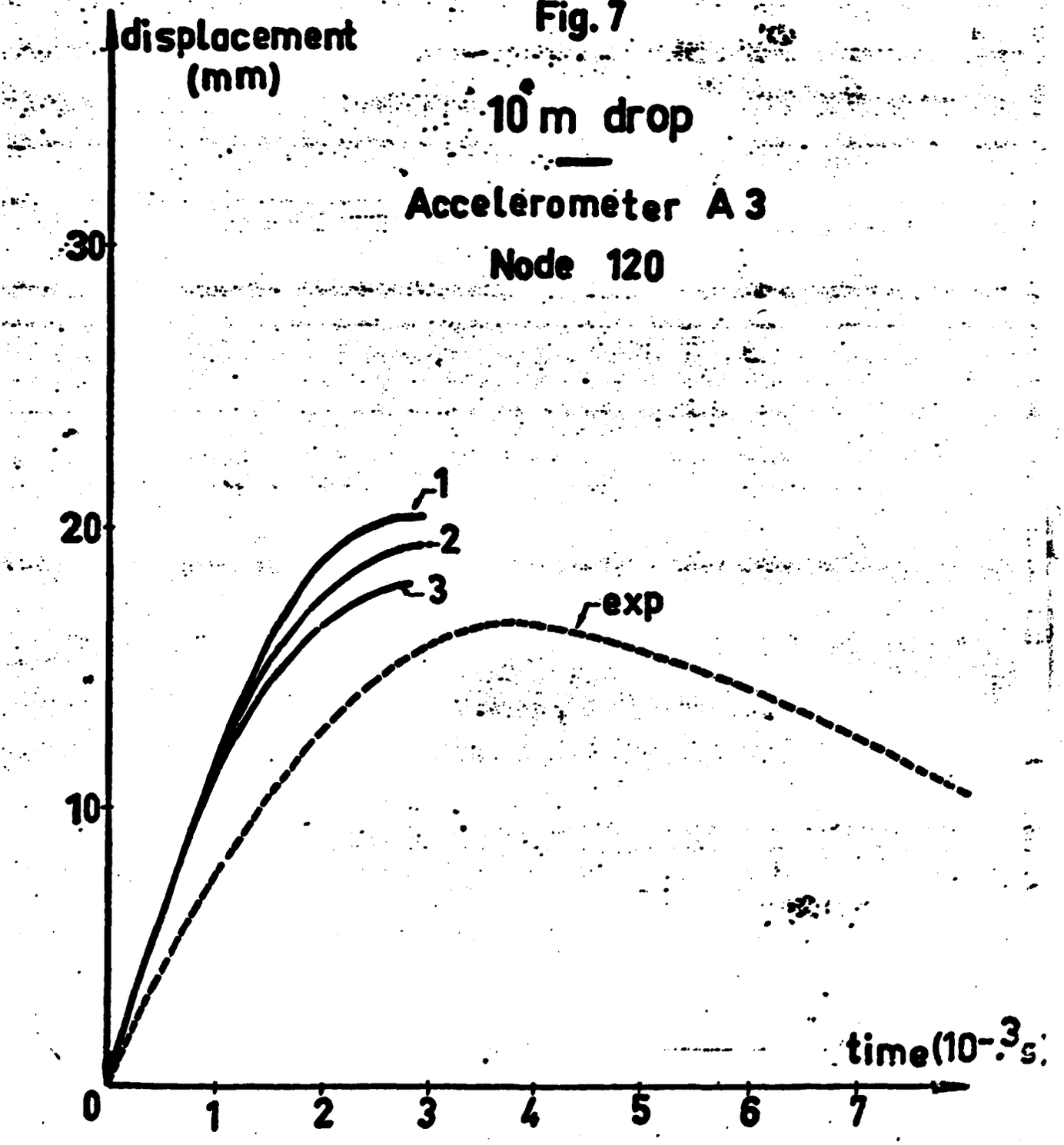
displacement
(mm)
10 m drop
Accelerometer A 3
Node 120
30
20
10
0
1
2
3
exp
time(10⁻³s)
1
2
3
4
5
6
7

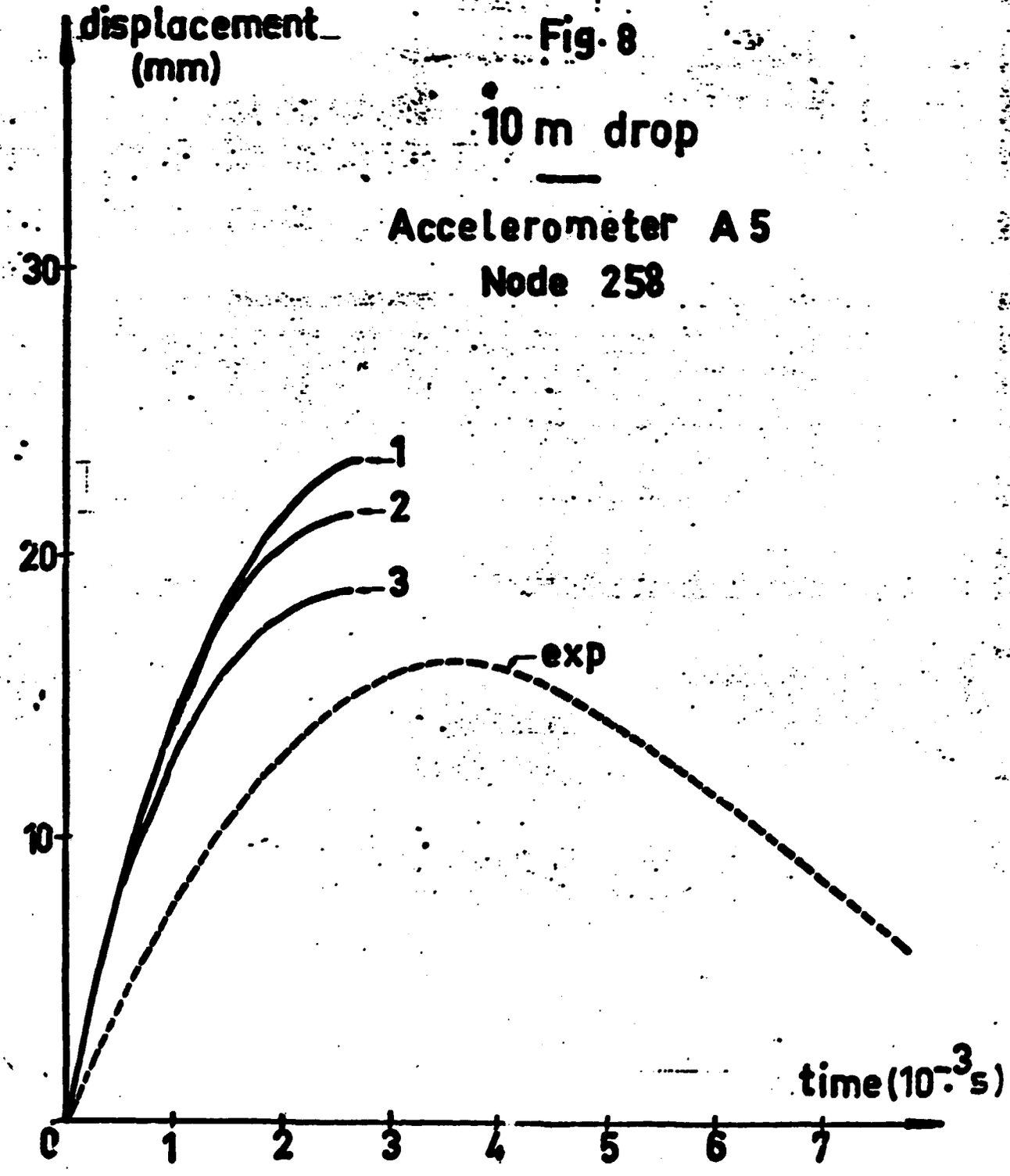
displacement (mm)
Fig. 8
10 m drop
Accelerometer A 5
Node 258
30
20
10
1
2
3
exp
time (10^{-3} s)
0
1
2
3
4
5
6
7

Fig. 9

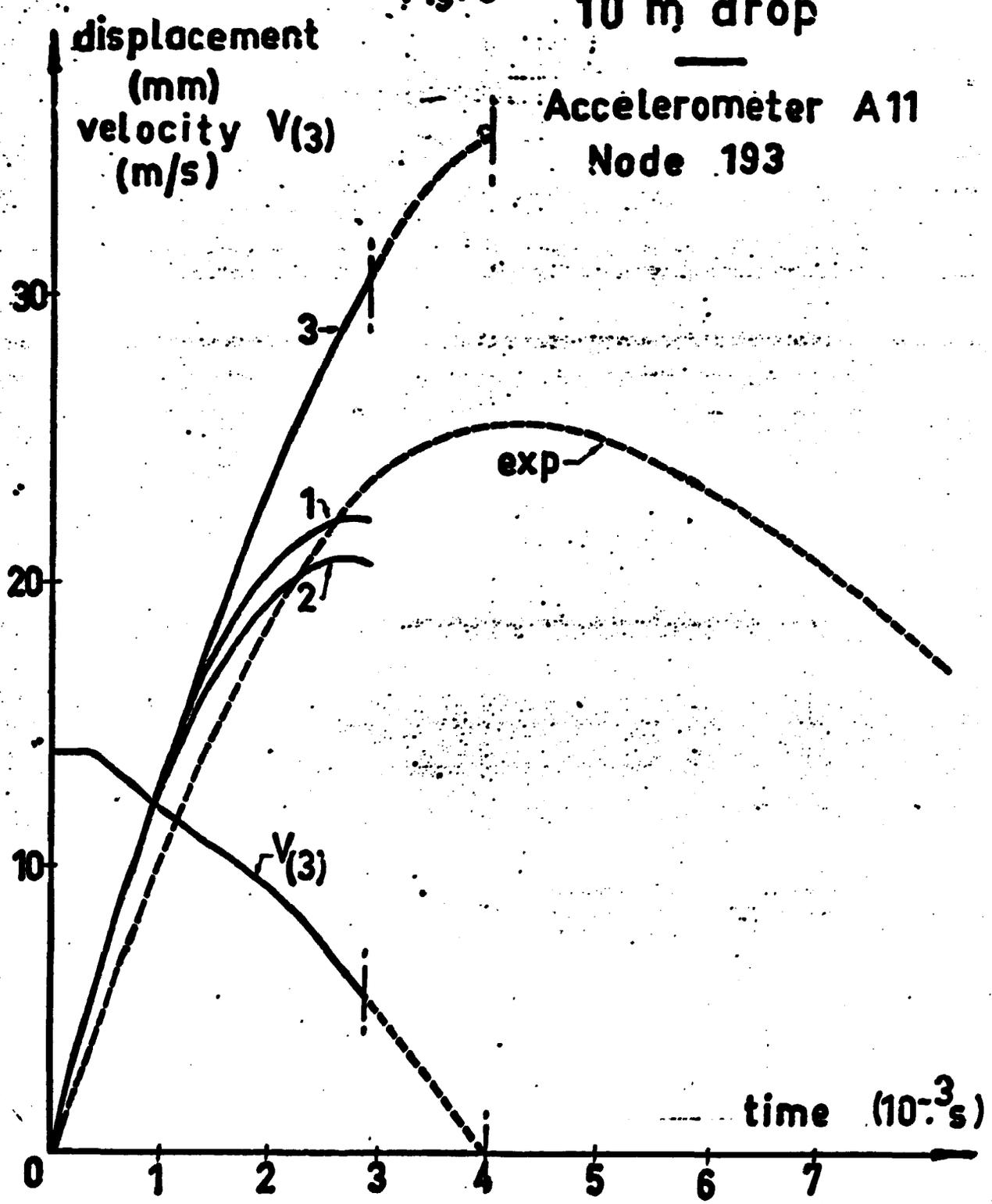
10 m drop
Accelerometer A11
Node 193
displacement
(mm)
velocity V(3)
(m/s)
30
20
10
0
3
exp
1
2
V(3)
time (10⁻³s)
1
2
3
4
5
6
7

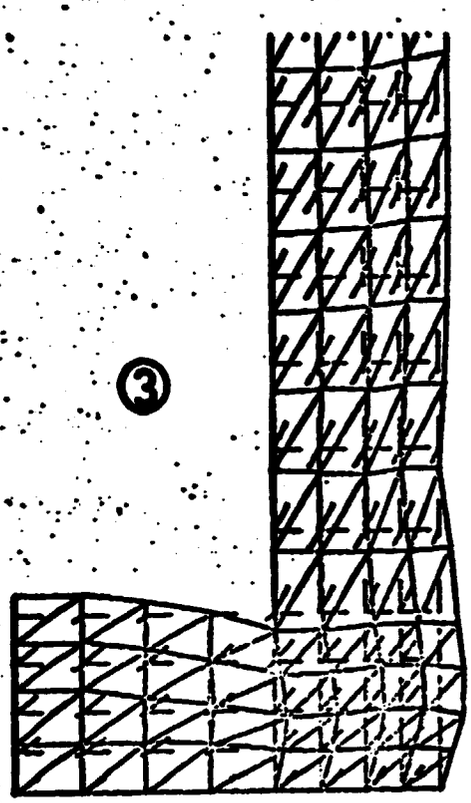

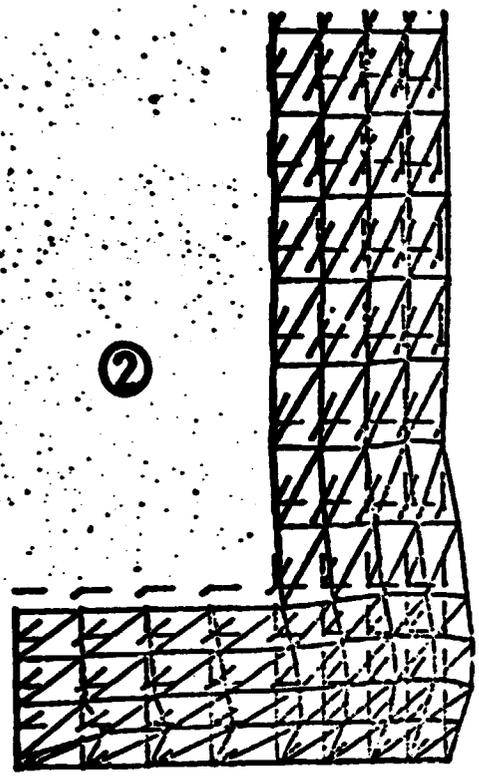

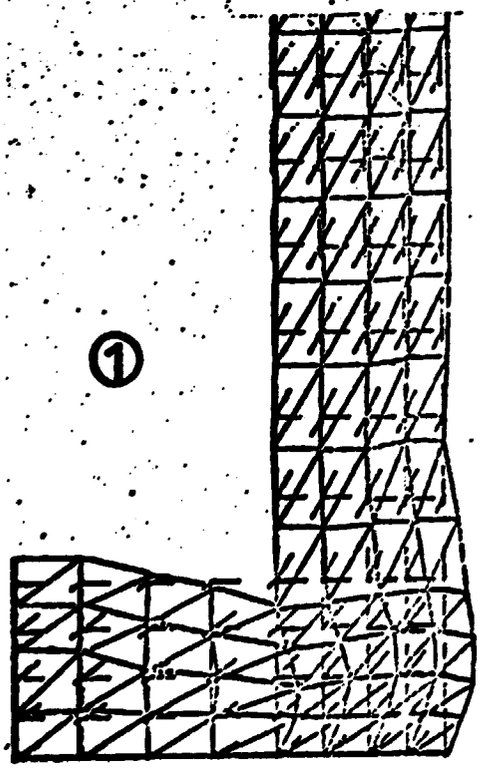

Fig. 10

10 m drop

Calculated deformations

with mod 1, 2 and 3

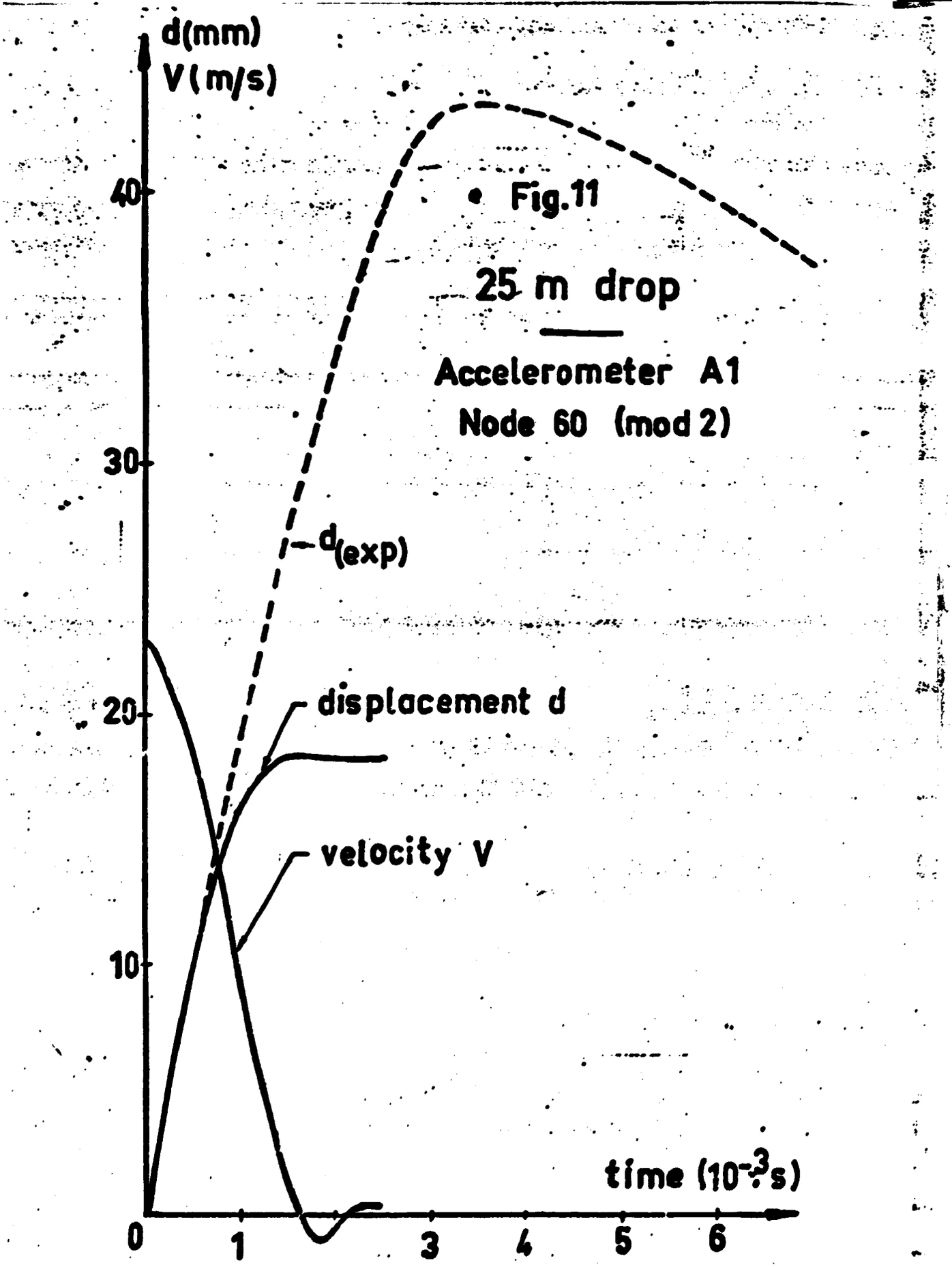
d(mm)
V(m/s)
40
30
20
10
0
1
3
4
5
6
time (10^{-3}s)
$d_{(exp)}$
displacement d
velocity V
25 m drop
Accelerometer A1
Node 60 (mod 2)

Fig.11

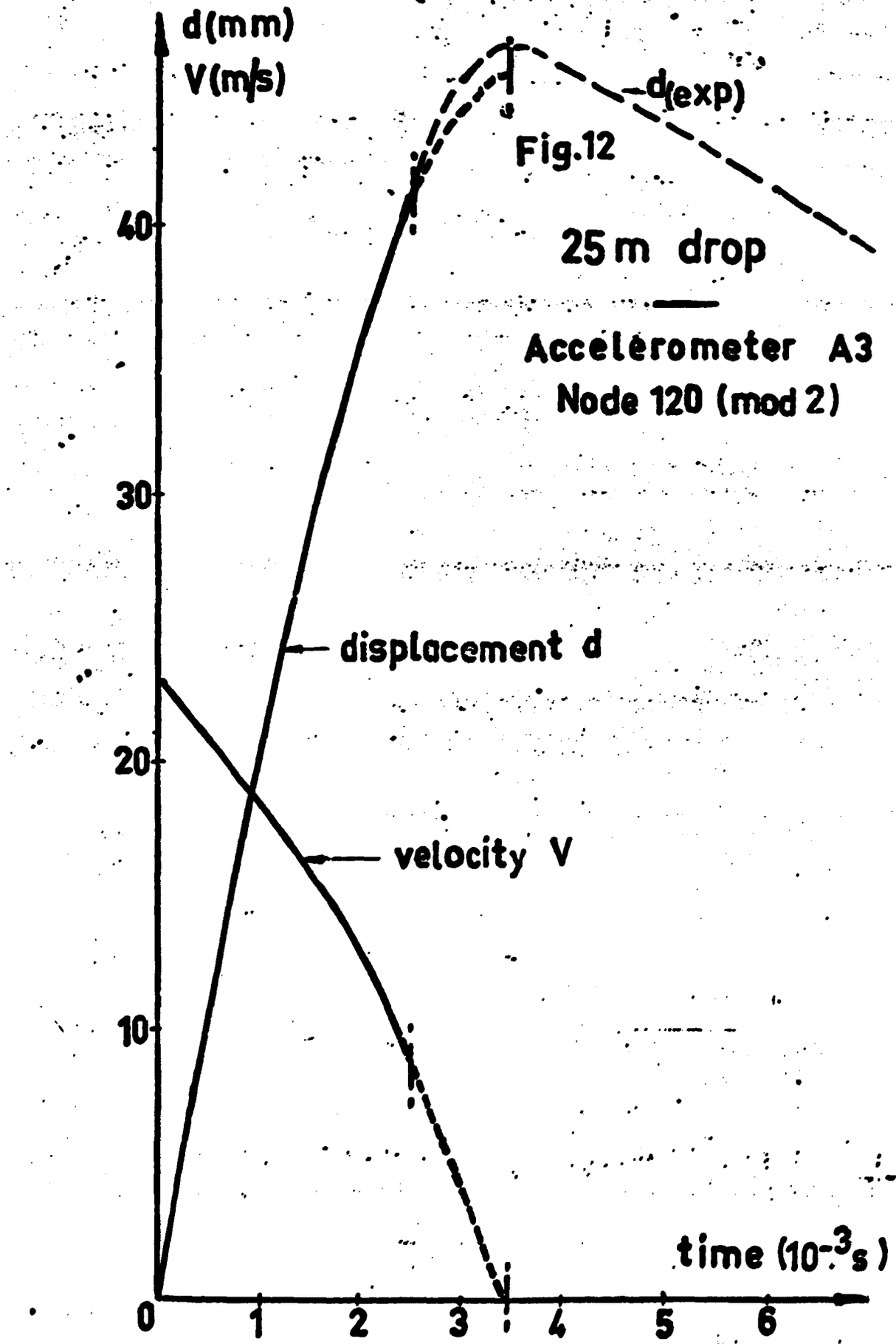
d(mm)
V(m/s)
d(exp)
Fig.12
25 m drop
Accelerometer A3
Node 120 (mod 2)
40
30
20
10
displacement d
velocity V
time (10^{-3}s)
0
1
2
3
4
5
6

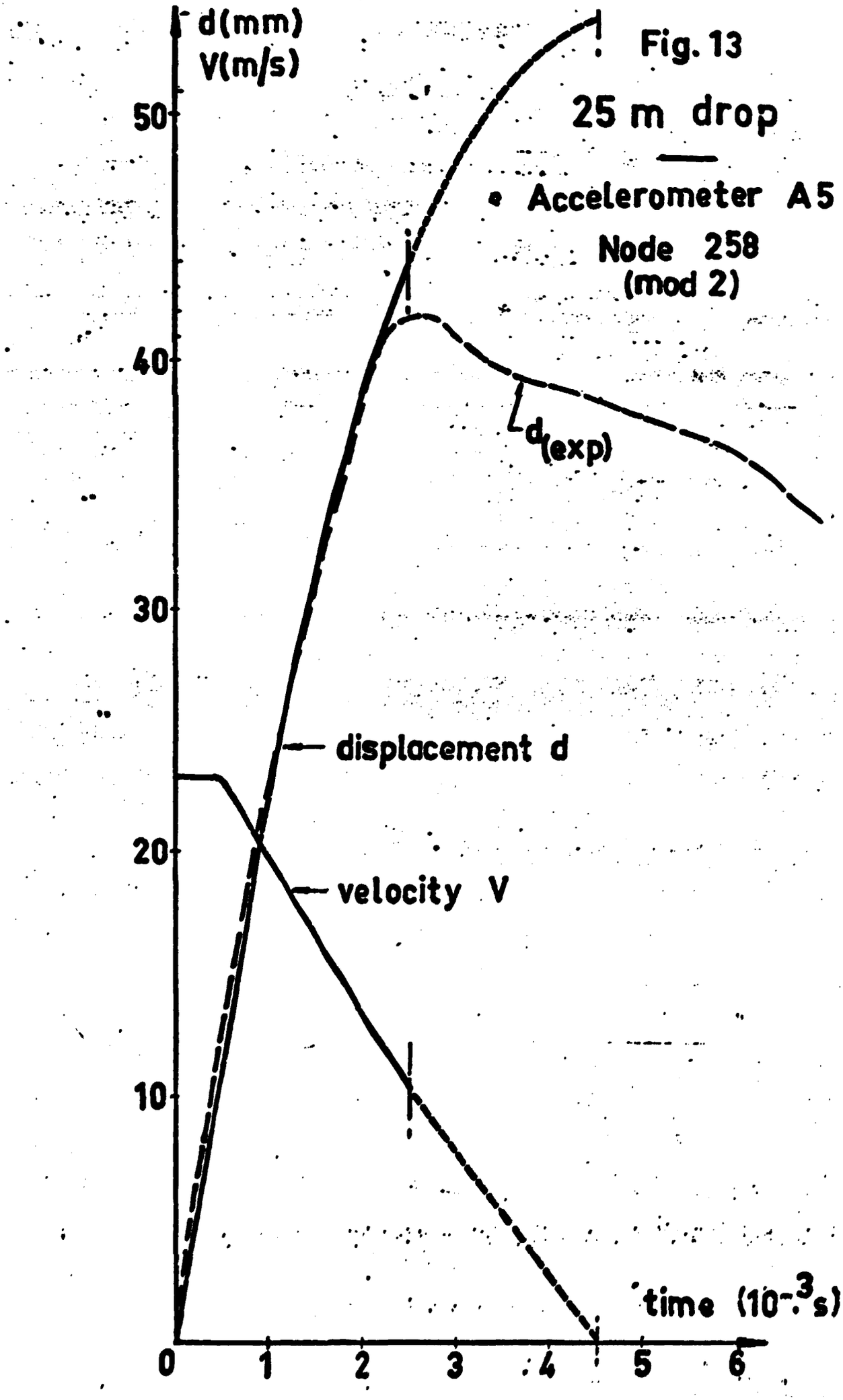
d(mm)
V(m/s)
50
40
30
20
10
0
1
2
3
4
5
6
Fig. 13
25 m drop
• Accelerometer A5
Node 258
(mod 2)
d(exp)
displacement d
velocity V
time (10⁻³s)

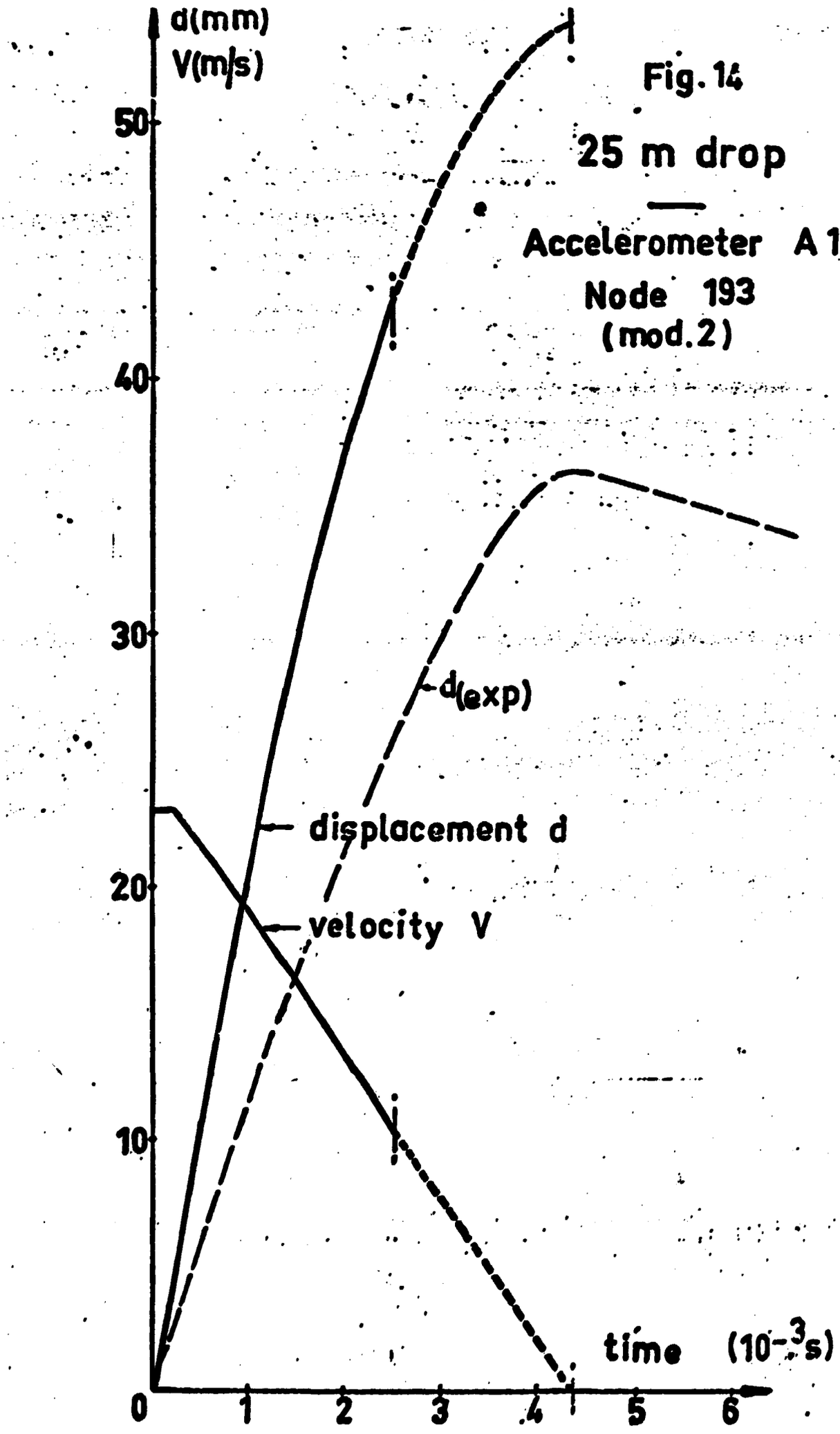

Fig. 14

25 m drop

Accelerometer A 11

Node 193

(mod.2)

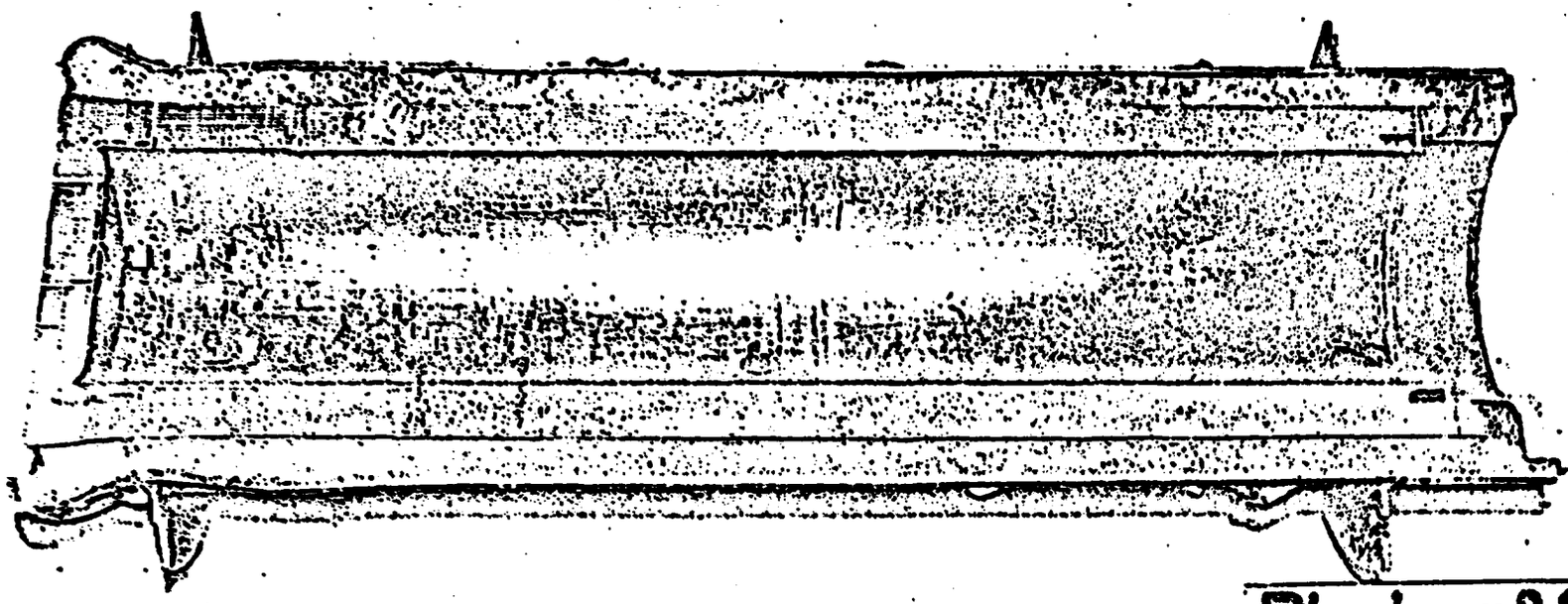

Photo n° 2

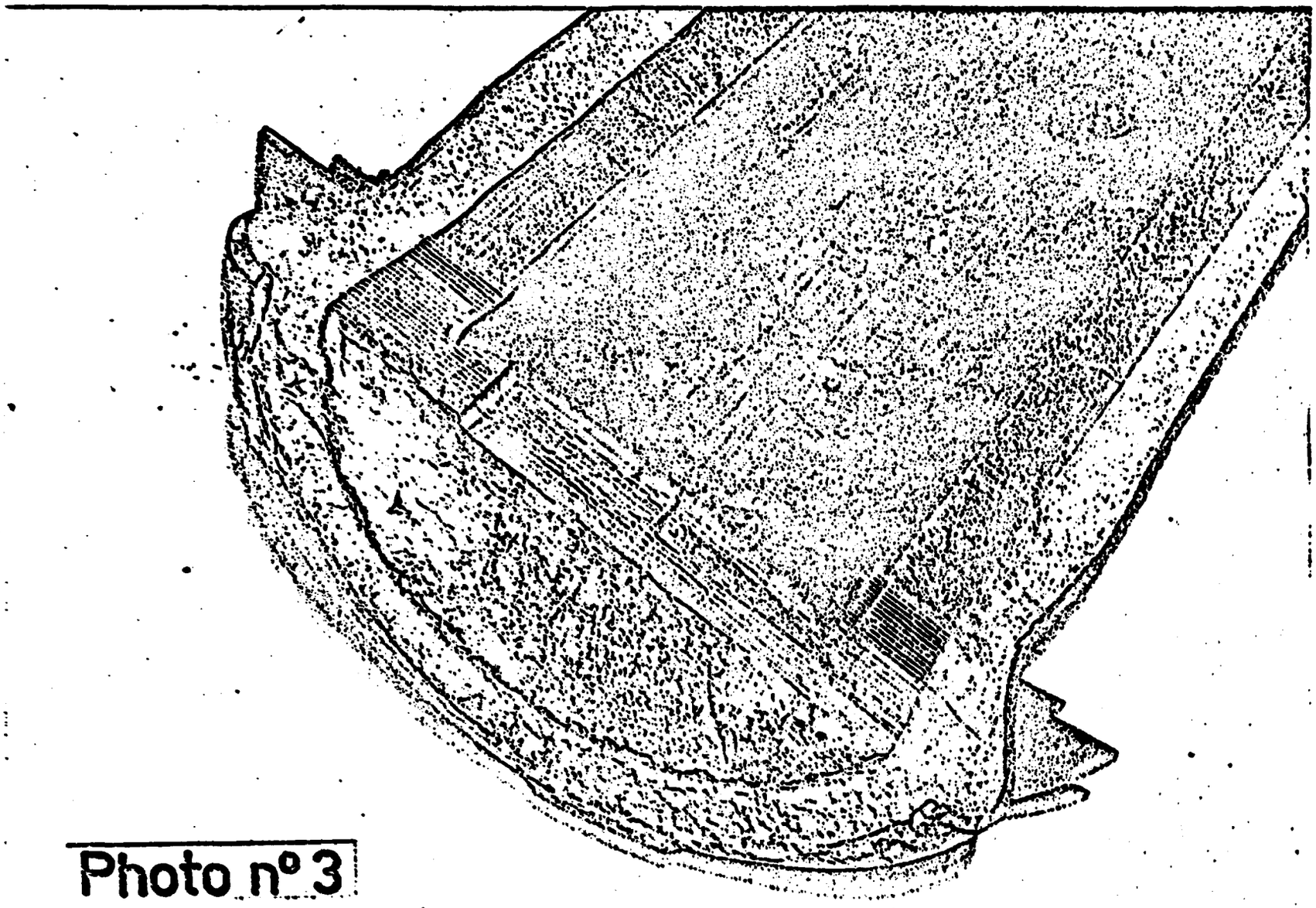

Photo nº 3

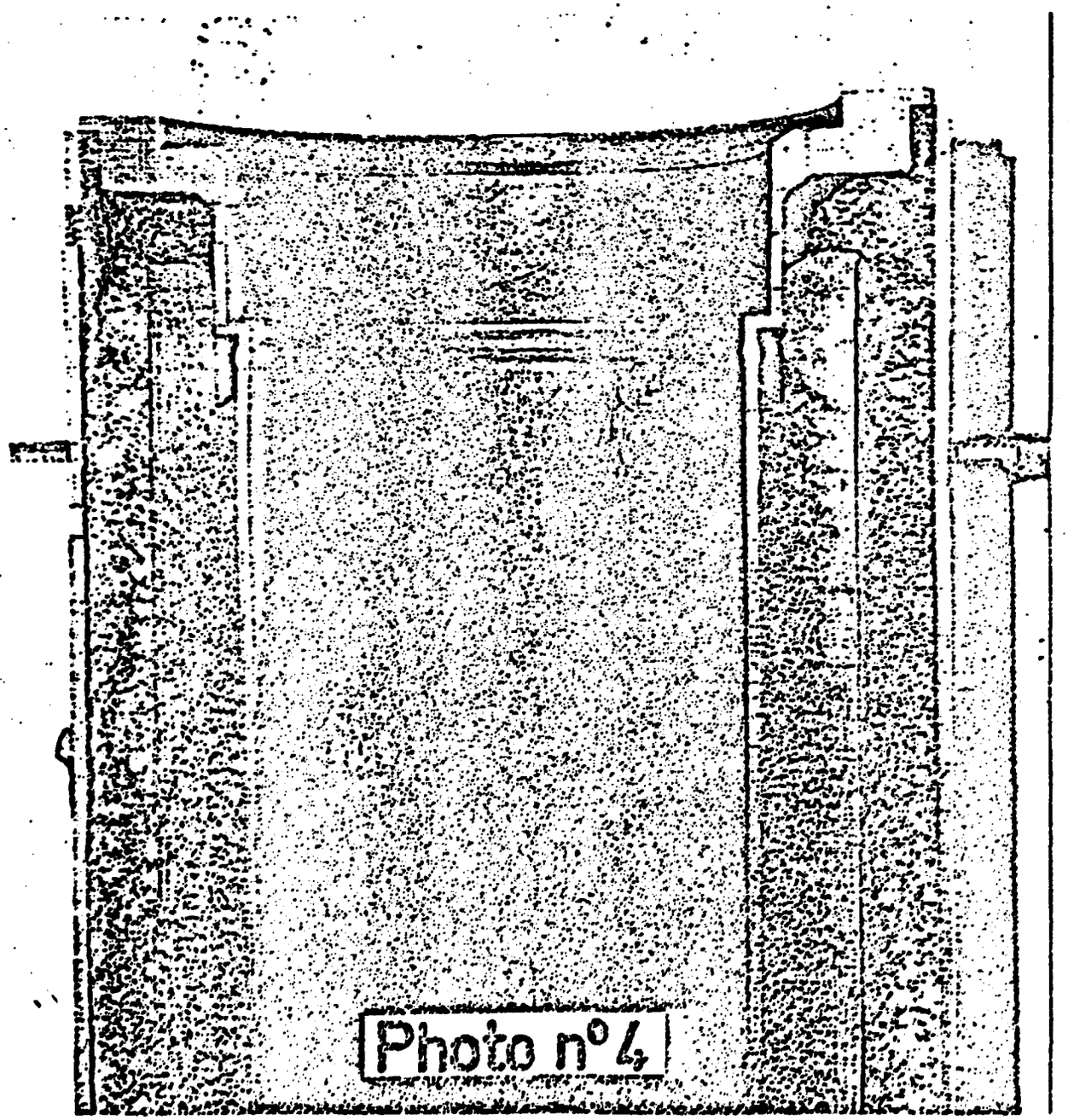

Photo n°4